Hypoxia-Regulated Activity of PKCε in the Lens

Vladimir Akoyev, Satyabrata Das, Snehalata Jena, Laura Grauer, and Dolores J. Takemoto

Purpose. To show that hypoxia is necessary to prevent opacification of the lens. Protein kinase C (PKC)-ε serves a role that is distinct from PKC-γ when both PKC isoforms are expressed in the lens. PKCε serves a very important role in hypoxic conditions, helping to prevent opacification of the lens.

Methods. Digital image analysis, confocal microscopy, dye transfer assay, coimmunoprecipitation, Western blot analysis, and enzyme activity assays were used, respectively, to study opacification of the lens, intercellular communications, cellular localization of connexin-43 (Cx43), and the interactions between PKCε, PKCγ, and Cx43 in the lens epithelial cells.

Results. Hypoxic conditions (1%–5% of oxygen) were very important in maintaining clarity of the lenses of wild-type (WT) mice. Normoxic conditions induced opacification of the WT lens. Lenses from the PKCε-knockout mice underwent rapid opacification, even in hypoxic conditions. Hypoxia did not induce apoptosis in the lens epithelial cells, judging by the absence of active caspase-3, and it did not change intercellular communication and did not affect the number and localization of junctional Cx43 plaques in the lens epithelial cell culture. Hypoxia activated PKCε, whereas phorbol ester (TPA), oxidation (H_2O_2), and insulin-like growth factor-1 (IGF-1) activated PKCγ and decreased the activity of PKCε. Hypoxia did not induce the phosphorylation of the Cx43.

Conclusions. Hypoxia-induced activation of PKCε is very important in surviving hypoxia and maintaining the clarity of the lens. However, PKCγ is utilized in the control of Cx43 gap junctions. (*Invest Ophthalmol Vis Sci.* 2009;50:1271–1282) DOI:10.1167/iovs.08-2599

The lens is a naturally hypoxic tissue.[1–4] Many studies have demonstrated that oxygen concentration in the lens is below 5% in the cortical region and around (or below) 1% in the nucleus.[2,3,5–7] The existence of these hypoxic conditions, which are pathologic for any other tissue brings up many questions about possible mechanisms by which the lens is able to accommodate hypoxia and maintain the subtle balance between apoptosis and differentiation. The lens has very low energy requirements, utilizes anaerobic glycolysis, and has a very low oxygen consumption rate (0.5 mL O_2/mg tissue dry weight/h) when compared to the cornea (2 mL), heart (5 mL), and retina (31 mL).[8,9] But the very low-energy requirement of the lens does not explain how the hypoxic lens overcomes all adverse affects of hypoxia. A partial answer may be found by drawing a comparison between lens and the well-known phenomenon of hypoxic preconditioning in the heart. In the heart, as has been shown many times, one of the mechanisms of cardiac protection against ischemia/hypoxia is based on stress-sensing PKC isoforms, including PKCε.[10] During myocardial ischemia connexin-43 (Cx43) is dephosphorylated,[11–19] and this is believed to allow gap junctions to be opened and to convey the propagation of ischemia injury.[20–23] Such adverse propagation of the ischemia signal can be mollified by many factors that specifically activate PKCε in the heart, such as ischemic preconditioning, FGF-2,[24–26] exogenous addition of TPA,[25,27–29] or hydrogen peroxide.[30] During ischemic preconditioning, PKCε plays a cardioprotective role through several mechanisms, such as: reduction of the intracellular Ca^{2+},[31] activation of the mitochondrial cytochrome *c* oxidase,[32–34] and phosphorylation of Cx43.[13,16,35] In the heart, in hypoxic conditions, PKCε is activated and migrates to membrane Cx43 gap junctions as well as to mitochondria, and, this process is essential for protection from ischemia.[36] The activated PKCε interacts with and phosphorylates Cx43, which aids in the propagation of ischemic injury.[21,25,35] In the mitochondria, PKCε interacts with mitochondrial cytochrome *c* oxidase (CytCOxIV), reduces the loss of CytCOxIV,[27,37,38] and helps prevent mitochondria-induced apoptosis.[39–41] In general, all these mechanisms inhibit ischemia–reperfusion damage[33] and are associated with cardioprotective effects of ischemic preconditioning on infarct size.[42,43]

Unlike cardiac tissue, lens tissue is naturally hypoxic and contains two stress-sensing PKC isoforms: PKCε and PKCγ.[44,45] As for PKCγ, it is very well known that it controls gap junction Cx43 through phosphorylation in many cell types.[46–48] Recently, we demonstrated that the specific ability of PKCγ to phosphorylate Cx43 allows PKCγ to block the propagation of apoptotic signals.[45,49] The role of PKCε in the lens is still unclear. Taking into account the role of PKCε in the heart, we recently studied the ability of hypoxia to regulate the PKCε in the lens. We found that in the lens, like in the heart, hypoxia activates PKCε which is associated with CytCOxIV in the mitochondria.[50] We also demonstrated that hypoxia-induced activation of CytCOx in the lens is PKCε dependent: Hypoxia not only activated PKCε but also stimulated interaction with CytCOx, which was not observed in lenses from the PKCε knockout mice (KO). However, it is not certain what role PKCε plays in the control of lens homeostasis. This work was directed to identifying that role.

Materials and Methods

Dulbecco's modified Eagle's medium (DMEM; low glucose), trypsin-EDTA, gentamicin, and penicillin/streptomycin were purchased from Invitrogen Corp. (Carlsbad, CA). Dithiothreitol (DTT), sodium fluoride (NaF), and bovine serum albumin (BSA) were purchased from Fisher Scientific (Hampton, NH). Fetal bovine serum was purchased from Atlanta Biologicals (Norcross, GA). Human recombinant FGF-2 (bFGF; cat. no. F0291), IGF-1 (cat. no. I3769), H_2O_2 (cat. no. H1009), phenylmethylsulfonyl fluoride (PMSF), and protease inhibitor cocktail (cat.

From the Department of Biochemistry, Kansas State University, Manhattan, Kansas.

This is publication number 08-226-J from the Kansas Experimental Station.

Supported by National Eye Institute EY0R01-13421 (DJT); National Institutes of Health Grant P20 RR016475 from the INBRE (Institutional Development Award [IDeA] Network of Biomedical Research Excellence) Program of the National Center for Research Resources (LG, DJT); and a grant from the Kansas City Life Science Institute (DJT).

Submitted for publication July 22, 2008; revised October 17, 2008; accepted January 15, 2009.

Disclosure: **V. Akoyev**, None; **S. Das**, None; **S. Jena**, None; **L. Grauer**, None; **D.J. Takemoto**, None

The publication costs of this article were defrayed in part by page charge payment. This article must therefore be marked "*advertisement*" in accordance with 18 U.S.C. §1734 solely to indicate this fact.

Corresponding author: Dolores J. Takemoto[b], Department of Biochemistry, 141 Chalmers Hall, Kansas State University, Manhattan, KS, 66506; dtak@ksu.edu.

no. P8340) were from Sigma-Aldrich (St. Louis, MO). TPA (cat. no. 524400), 4α-phorbol-12,13-didecanoate (PDD, cat. no. 524394), and phosphatase inhibitors cocktail set II (cat. no. 524625) were purchased from Calbiochem (La Jolla, CA). PKC activity nonradioactive assay kit (cat. no. EKS-420) was purchased from Stressgen (Ann Arbor, MI). Protein A/G plus agarose beads were purchased from Santa Cruz Biotechnology (Santa Cruz, CA). All electrophoresis reagents and protein molecular weight markers for electrophoresis and protein assay dye were purchased from Bio-Rad Laboratories (Hercules, CA). Chemiluminescence substrate (SuperSignal West Femto Substrate Kit) with secondary anti-mouse or anti-rabbit IgG conjugated with horseradish peroxidase (cat. no. 34095) was purchased from Pierce (Rockford, IL).

Animals

All animal procedures were approved by the Kansas State University Institutional Animal Care and Use Committee. Mice, including control and PKCε knockout (KO) mice, were obtained from Jackson Laboratories (Bar Harbor, ME) and maintained as colonies in the Animal Research Facility at the College of Veterinary Medicine. PKCε KO mice were obtained by breeding heterozygous individuals and the genotyping of the offspring was performed by PCR of tail snips. Yield was ~10% homozygous for the PKCε KO. The control mice were B6.129S4-Prkce/tm1/Msg/J and the PKCε heterozygous mice (with or without PKCε) were Prcke/tm1/Msg-2-3. Only homozygous KO-PKCε mice were used from cross-breeding of heterozygous pairs. All mice were used at 6 weeks of age. The failure of the $PKC\varepsilon^{-/-}$ mice to produce PKCε protein was further verified by Western blot analysis with PKCε antisera. The mice were killed by CO_2 followed by cervical dislocation. All experiments conformed to the ARVO Statement for Use of Animals in Ophthalmic and Vision Research.

Lens Culture

The eyeballs were surgically removed immediately after death and placed on ice. Immediately after eye surgery they were dissected in the microscope, and the lenses were placed in DMEM (with 10% serum) without phenol red, previously equilibrated with 1% O_2 and 5% CO_2 (hypoxic DMEM) for 12 hours and then washed twice with the same media to remove vitreous and pigmented tissue. Average time required for dissection during which lenses were exposed to air was 15 seconds. Twelve lenses were used for every experimental data point regardless of left or right eye, color of the eyeballs, size of the lens, or the sex of the mice. All lenses for every experimental data point were collected after dissection into one Petri dish and were washed together, and then 12 randomly chosen clear lenses were transferred into a new Petri dish (50 mm) covered with 2 mL of hypoxic DMEM and placed in the hypoxic chamber. Lenses with visible damage were discarded.

Analyses of Opacification

After an appropriate incubation time, the Petri dishes with the 12 lenses were taken out of the chamber and lens opacification was assessed by photographing the lenses with a digital camera according to Behndig et al.[51] Briefly, to assess opacification, the 256-level gray-scale photographs of the steel grid (8 lines/mm) were taken through the lens by using retroillumination. Every picture taken for the analyses contained clear grid, background, and lens. The analyses of opacification were conducted with digital image-analysis software (ImageJ, a public domain, Java-based image processing program developed in the National Institutes of Health, Bethesda, MD; available at http://rsb.info.nih.gov/ij/index.html.) by marking a circular area of 0.8 mm^2 (1 mm in diameter) of the grid, background, and lens on the photograph and calculating a histogram of the distribution of gray values. The theoretical zero opacity, which is equal to the maximum transparency, was determined from the image of the grid alone, without the lens. Most of the pixels of the grid image are black and white, which renders a very broad histogram with a standard deviation (SD_{zero}) of ~50.00 (Fig. 1A). This value of SD_{grid} was calculated for every image separately and used as the theoretical zero opacity. The image of the background that gives uniform gray pixels values with a very small SD (SD_{bkg} ~1.0) and a sharp histogram (Fig. 1B) gives a value of theoretical maximum opacity. The experimental opacity of the lens was achieved by calculating a histogram and SD (SD_{exp}) of the distribution of gray values of the grid visible through the lens (Fig. 1C). After that, the opacity of the lens was expressed as a percentage of the theoretical zero opacity: $100 \times SD_{exp}/SD_{zero}$. To minimize the difference between photographs, we placed all lenses from one experimental set simultaneously on the grid, and several pictures were immediately taken. To minimize the difference between control and KO lenses, we photographed control and KO lenses together on the same grid. Freshly isolated lenses from control and KO mice are always clear; however, since murine lenses have a distinct biconvexity it was not possible to get a perfectly focused image of the grid for the central and periphery (close to equatorial region) parts of the lens at the same time. An unfocused image of the grid contains significantly more gray pixels and therefore significantly smaller SD_{exp}. To minimize the contribution of the unfocused peripheral parts of the lens on the final histogram and SD_{exp}, we used five different circular focus areas of 0.8 mm^2 (1 mm in diameter): central, left, right, top, and bottom. Five photographs with

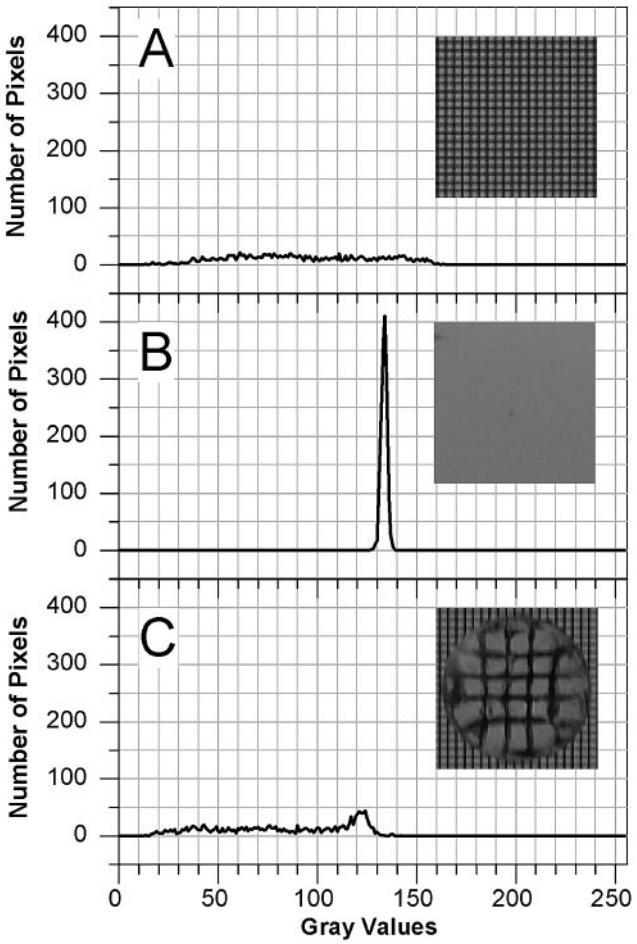

FIGURE 1. (**A**) Theoretical zero-opacity histogram: the *x*-axis represents the gray-scale values and the *y*-axis shows the number of pixels found for each gray value. The theoretical zero opacity that is equal to the maximum transparency was determined from the image of the grid alone (*inset*), without lens. Circular area of 0.8 mm^2 (1 mm in diameter) of the grid on the photograph was used for analyses. Most of the pixels are black and white, which renders a very broad histogram with SD ~ 50.00. (**B**) The theoretical maximum (100%). Opacity was determined from the image of the background that gives uniform gray pixels values with a very small SD_{bkg} ~ 1.0 and a sharp histogram. (**C**) Experimental opacity of the lens: analysis of experimental opacification was performed by calculating a histogram of the distribution of gray values of the grid visible through the lens.

five different focuses on the central, top, bottom, and left–right areas were made and used for histogram calculations.

Antisera

Mouse monoclonal anti-N-terminal-Cx43 IgG (cat. no. Cx43NT1) and anti-C-terminal-Cx43 (cat. no. Cx43IF1) were from the Fred Hutchinson Cancer Research Center (Seattle, WA); rabbit polyclonal anti-phospho-Cx43 (Ser-368; cat. no. 3511S) from Cell Signaling Technologies (Danvers, MA); mouse anti-PKCγ IgG (against C-terminal amino acids 449-697 region, cat. no. P20420) and mouse anti-PKCε-Ser729 from Transduction Laboratories (Lexington, KY); rabbit polyclonal anti-PKCε IgG (cat. no. 06-991) from Upstate Biotechnology (Lake Placid, NY); mouse anti-β-actin ascites fluid (cat. no. A5441) from Sigma-Aldrich; mouse anti-α-tubulin monoclonal IgG (cat. no. 32-2500) from Zymed-Invitrogen (San Francisco, CA); rabbit anti-active caspase-3 monoclonal IgG (cat. no. 559565) from BD Biosciences (San Jose, CA); mouse anti-HIF-1α monoclonal antibody from Novus Biological (Littleton, CO); and Alexa Fluor 488 goat anti-mouse or anti-rabbit IgG (H+L) conjugated secondary antibodies, and anti-fade reagent (cat. no. P36934; ProLong Gold) from Invitrogen-Molecular Probes (Eugene, OR).

Tissue Culture

Rabbit lens epithelial cells (NN 1003A) or human lens epithelial cells were grown in DMEM with 10% fetal bovine serum (FBS) until 100% confluent in normoxic conditions unless otherwise specified (described later). The cells were used for experiments at 100% confluence on the third day after the last split. They were starved in DMEM without fetal bovine serum for 4 hours before treatment with growth factors, TPA, or H_2O_2. They were then treated at 37°C for 30 minutes with stress factors such as H_2O_2 (100 μM) and TPA (200 nM) and growth factors such as FGF-2 and IGF-1 (both at 25 ng/mL) by direct adding of the aforementioned substances to the medium. PDD was used as a negative control for TPA treatment.

Hypoxia

Normoxic conditions, or normoxia, were considered to be a state in which the partial pressure of oxygen in the gas is equal to that of air at sea level—approximately 21% oxygen or 150 mm Hg—plus 5% CO_2 at 37°C and 100% relative humidity in a cell culture incubator. Hypoxic conditions were created with the help of a hypoxic chamber (Proox C21; BioSpherix, NY) using nitrogen and CO_2 as displacement gases, set at 1%, 3%, 5%, and 10% O_2; 5% CO_2; 37°C; and 100% relative humidity. Petri dishes (100 mm) and 10 mL of DMEM (10% FBS) were used for cell culture, to ensure appropriate and fast ventilation of cultures in the chamber. No changes in the pH of the cell media were registered during hypoxia incubation for up to 4 days, as assessed by direct measurements of pH of the media in the dishes. Immediately after surgery, the mouse lenses were incubated in the DMEM (10% serum without phenol red) for 4, 8, or 12 hours in different oxygen concentrations (1%, 3%, 5%, 7%, or 10%, or 21% for normoxia), plus 5% CO_2 at 37°C and 100% relative humidity.

Whole-Cell or Lens Lysate Preparations

To reduce oxygen exposure during cell lysate preparations, after hypoxia experiments, phosphate-buffered saline (PBS) and cell lysis buffer were degassed for 30 minutes in a vacuum before experiments. Immediately after hypoxia treatment, cells were washed with 37°C PBS, collected from Petri dishes by scraping, sedimented, and washed two times in PBS. The cell pellets were lysed on ice with cell lysis buffer containing 20 mM Tris-HCl (pH 7.5), 0.5 mM EDTA, 0.5 mM EGTA, 1% Triton X-100, protease inhibitor cocktail (1:100), 2 mM PMSF, and phosphatase inhibitor cocktail (1:100). The lysates were sonicated for 20 seconds on ice. Protein concentration was equalized in all samples for future analyses.

Western Blot and Coimmunoprecipitation Analyses

Western blot and immunoprecipitation analyses of cell lysates followed by Western blot analyses were performed as previously described.[52] All cell lysates had the same total protein concentration (2 mg/mL) before immunoprecipitation. Anti-PKCγ, anti-PKCε, and anti-Cx43-NT1 antibodies at 5 μg/mL were used for immunoprecipitation.

PKC Enzyme Activity Assays

PKC activity was determined by use of a PKC activity assay (Stressgen). Cell lysates from separate experiments were divided into three aliquots to run assays in triplicate for statistical purposes. Each was immunoprecipitated with anti-PKCγ or anti-PKCε antibodies as described previously.[52] The immunoprecipitate-agarose bead complexes were used directly to measure the activity of each PKC isoform according to the manufacturer's manual. Three separate experiments were performed to obtain statistically relevant data. Purified recombinant active PKC supplied by the manufacturer was used as a positive control. Cell lysis buffer alone, supplemented with primary antibodies and agarose beads was used as a blank for the enzyme assay. Because of unavoidable variations in absolute values of PKC activity in separate experiments the final values of activities for all samples were normalized using the PKCγ control as a 100% for each experiment. Normalization of data to PKCγ control levels allowed the direct comparison of separate datasets regardless of the absolute values. Phosphatase inhibitors were present in all procedures, so that PKCγ and -ε autophosphorylation and the resulting activation could be maintained.

Confocal Scanning Fluorescent Microscopy

To visualize the specific location of Cx43 in the cells before and after the treatments, confocal scanning fluorescent microscopy was used, as previously described.[52] Lens cells were grown on coverslips, treated as described earlier and then fixed in 4% paraformaldehyde, permeabilized, blocked, and treated with primary anti-Cx43-IF1 antibodies at 5 μg/mL concentration as previously described.[52] Secondary fluorescent Alexa Fluor-488 antibodies at 10 μg/mL were used to visualize the specific location of the primary antibodies,.

Dye Transfer–Gap Junction Activity Assay

To study the gap junction activities in cell culture the scrape-loading/dye transfer (SL/DT) assay with lucifer yellow and rhodamine dextran was performed as described before.[44,53,54] Gap junction activity was expressed as the number of cells transferring lucifer yellow minus cells with rhodamine dextran per total number of DAPI-stained cells. Three different areas along each scrape were analyzed with at least 1000 cells counted. The number of cells transferring lucifer yellow were expressed as the mean ± SD, with $P < 0.05$ considered significant.

Statistical Analyses

Commercial software (Origin; Microcal Software Inc., Northampton, MA) was used for statistical analyses. Results were expressed as the mean ± SD. Differences at $P < 0.05$ were considered to be statistically significant.

Results

Lens Opacification Study

To investigate the effects of hypoxia on PKCε, we had to establish the main physiological outcome/property that is relevant for the lens. This property is the transparency of the lens and its opposite characteristic, opacity of the lens. Wild-type lenses and lenses from PKCε-KO mice were cultured together in the separate wells in hypoxic conditions at 1%, 3%, 5%, and 10% O_2 and in 21% O_2 (normoxia) for 4, 8, and 12 hours. Figure 2A shows representative images of the fresh wild-type (WT) and PKCε-KO lenses before incubation. Freshly isolated lenses

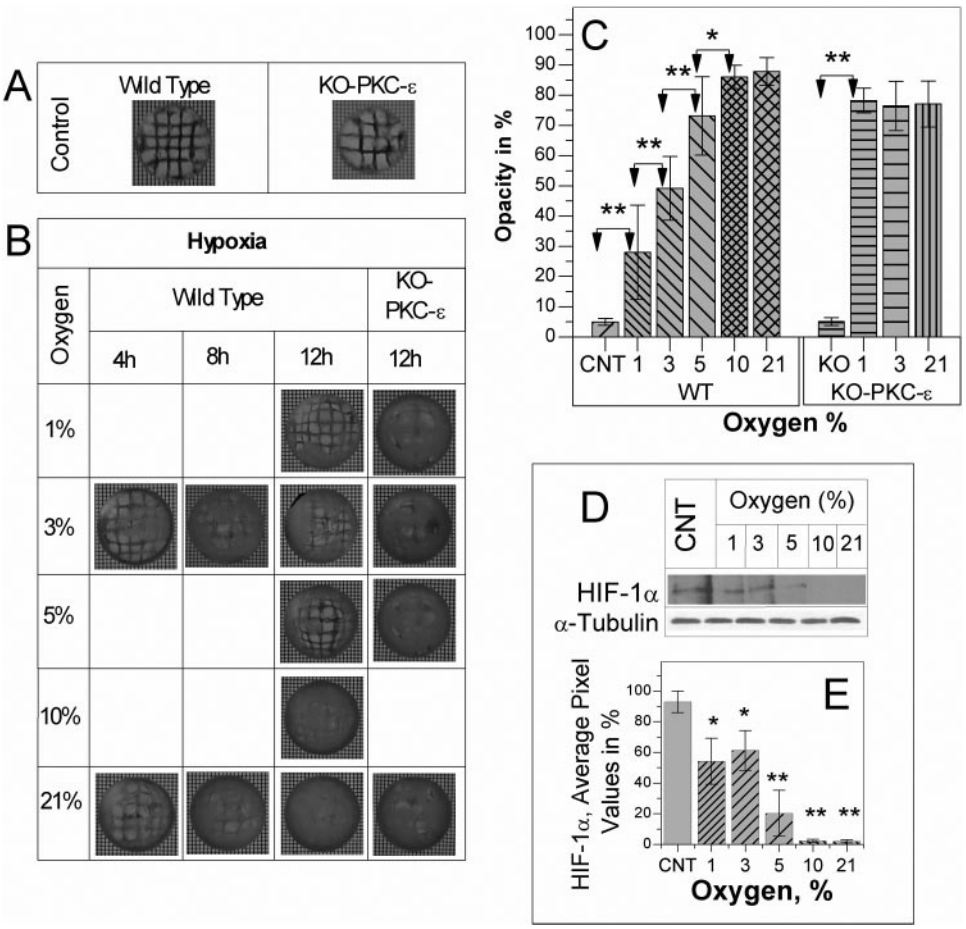

FIGURE 2. (**A**) Freshly isolated lenses from wild-type control and KO mice. (**B**) Images of the wild-type control and KO mice after 4, 8, and 12 hours of hypoxia in vitro. PKCε KO lenses show abnormal opacification in hypoxic conditions in vitro. (**C**) Experimental opacity of the lens is expressed as a percentage of the theoretical zero opacity. Fresh wild-type and KO lenses are always clear; however, since murine lenses have a distinct biconvexity and the experimental procedure obviously produced some optical defects, it was not possible to obtain values of the experimental opacity of the lens equal to zero. Therefore, the mean value of the experimental opacity of freshly isolated wild-type control (CNT) lenses was 4.9 ± 1.7 and the that of freshly isolated KO lenses was 5.1 ± 1.9 ($P > 0.05$). Data are plotted as the mean ± SD. Significant differences: $^{*}P < 0.05$); $^{**}P < 0.001$ between data indicated by *arrows*. There is no significant difference between values of mean experimental opacity for 10% and 21% oxygen in the WT group and between 1%, 3%, and 21% oxygen in the KO group. (**D**, **E**) Western blot analyses of HIF-1α in lens homogenates of freshly isolated wild-type lens (CNT) and lenses after hypoxia treatment. Increased levels of oxygen (10%–21%) induced the disappearance of HIF-1α. α-Tubulin was used as the loading control. The average pixel values (**E**) for every HIF-1α band were calculated and then normalized and plotted as a percentage of the control (CNT) value obtained in freshly isolated lenses. (Un-Scan-It gel and graph digitizing software was used to digitize the bands; Silk Scientific, Orem, UT).

from control and KO mice have always been clear; however, since murine lenses have a distinct biconvexity, and experimental procedure obviously produced some optical defects, it was not possible to obtain opacification value equal to zero. Opacity of the fresh WT lens and fresh PKCε-KO lens at the beginning of incubation was the same and did not exceed 5% (4.9 ± 1.1 for WT, and 5.1 ± 1.3 for KO, mean ± SD; Figs. 2B, 2C). Increased concentration of oxygen induced opacification (Figs. 2B, 2C). Wild-type lens became opaque at 21% oxygen, even after 4 hours of incubation (opacity, 68.16 ± 10.13) and stayed relatively transparent after 12 hours in 1% O_2 (opacity, 28.02 ± 15.61). Remarkably, that opacity of the WT lenses demonstrated gradual increasing from 1% to 10% oxygen, whereas PKCε-KO lenses became opaque up to 78%, even after 4 hours, regardless of the concentration of the oxygen (Figs. 2B, 2C). It is worth noting that careful visual examination of every lens in the microscope in all experiments demonstrated that in all cases opacification started from the equatorial region of the lens. Even during preliminary experiments when the apical and posterior parts of the lens were intentionally tapped with forceps during transfer to the Petri dishes, opacification started from the equatorial region. We did not do more careful studies of the lens, but at the level of the visual examination in a microscope we can make a conclusion that opacification was cortical and spread from the equatorial to the apical and posterior regions which were the last parts where opacification occurred (as well as the nuclear part of the lens). Although we took care to prevent exposure of all lenses to O_2, obviously some handling (~15 seconds) resulted in some exposure to oxygen. However, these results clearly demonstrated the following: hypoxia has a profound effect on the main physiological property (transparency) of the lens; hypoxia is the normal physiological state, and any condition close to normoxia promotes opacification; and PKCε is necessary for the protection of the lens from opacity. Fresh lenses as well as lenses incubated in hypoxic conditions for 12 hours demonstrated the expression of HIF-1α (Fig. 2D), and the level of HIF-1α normally seen in the hypoxic lens was decreased in normoxic conditions (Fig. 2E). Our hypothesis is that the high level of opacification in the PKCε-KO lens resulted, first, from the loss of PKCε–dependent activation of the CytCOxIV when the lens had brief normoxia due to handling. Previously, we demonstrated that PKCε is a prerequisite for hypoxia-induced activation of the CytCOxIV.[50] The second possibility may result from an effect of PKCε on Cx43 which is absent in PKCε-KO mice.

Effect of Hypoxia on Gap Junction Communication

To analyze the effect of hypoxia on gap junction Cx43 communication, we performed scrape-loading/dye transfer experiments using cultured human lens epithelial cell. Figures 3A and 3B show that hypoxia (1% up to 24 hours) did not inhibit dye transfer; thus, the dye transfer does not depend on oxygen concentration. This effect is opposite the effect of hypoxia on dye transport that has been observed in cultured cardiac myocytes.[55] To verify the hypoxic conditions in our experiments, we measured the expression of HIF-1α by Western blot analysis. Lens epithelial cells constitutively expressed HIF-1α in normoxic and hypoxic conditions (Figs. 3D, 3E). The second

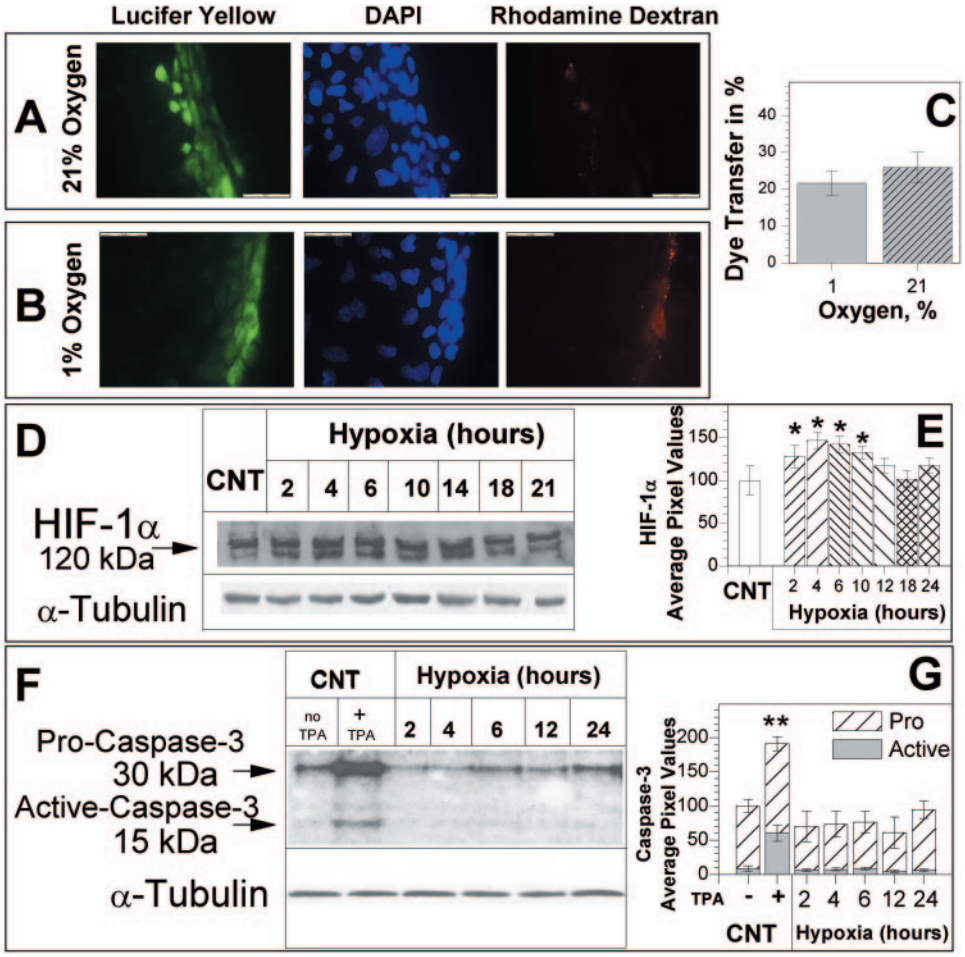

FIGURE 3. Scrape-loading/dye transfer analyses of the lens epithelial cells in (**A**) normoxic conditions and (**B**) after hypoxia (1% O_2 for 24 hours). (**C**) Dye transfer was expressed in percentages as the number of cells transferring lucifer yellow minus cells with rhodamine dextran per total number of DAPI-stained cells. (**D**, **E**) Western blot analyses of HIF-1α in cell lysates in normoxic (CNT) conditions (20% O_2, 5% CO_2, 37°C) and during hypoxia (5% O_2, 5% CO_2, 37°C). Average pixel values were calculated for both bands of HIF-1α. The second band of HIF-1α at 100 kDa represents post-translational modification of HIF-1α according to Reference 56. (**F**, **G**) Western blot analyses of caspase-3 in cell lysates in normoxic (CNT) conditions (20% O_2, 5% CO_2, and 37°C) and during hypoxia (5% O_2, 5% CO_2, and 37°C). TPA treatment (200 nM, 30 minutes, 37°C) was used as a positive control for active caspase-3. α-Tubulin was used as the loading control. Data are plotted as the mean percentage (±SD) of control ($n = 4$). Significant differences: $^*P < 0.05$; $^{**}P < 0.001$ between the indicated data and the control.

band of HIF-1α at 100 kDa, found during hypoxia (Fig. 3D), represents posttranslational modification of HIF-1α according to Gothie et al.[56] and the manufacturer of the HIF1α antisera (Novus Biologicals). We also found that lens epithelial cells did not undergo apoptosis, as determined by Western blot with anti-active caspase-3 antibodies in normoxic or hypoxic conditions (Figs. 3F, 3G). TPA treatment (200 nM, 30 minutes) was used as a positive control for active caspase-3 activation in the lens epithelial cells. These data demonstrated that hypoxia, in vitro, does not induce the apoptotic process and does not inhibit intercellular communication. Taking into account that Cx43 is responsible for dye transport in the cultured lens

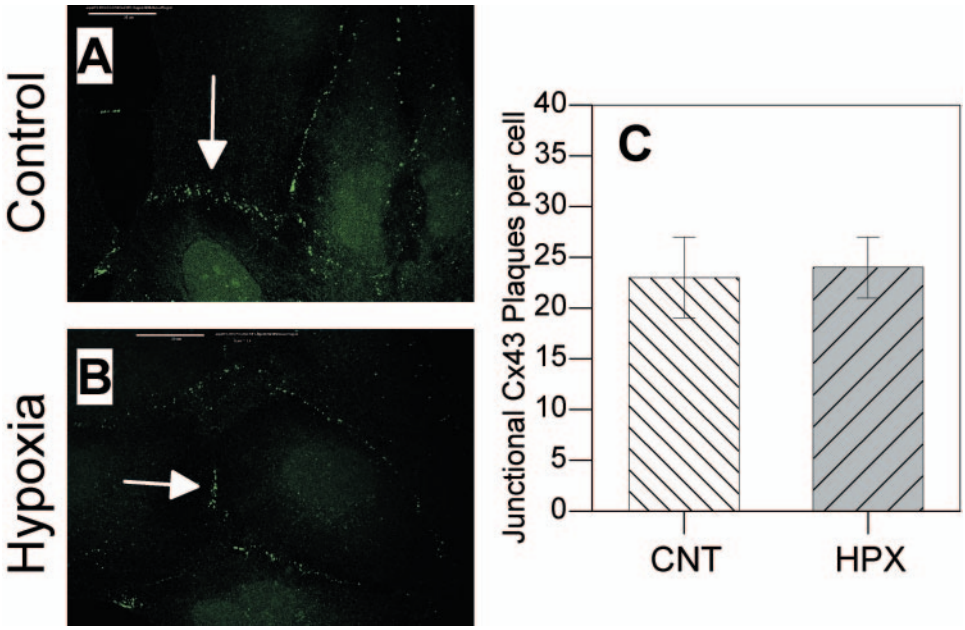

FIGURE 4. Confocal images of immunolabeled Cx43 in the human lens epithelial cells: (**A**) Control, normoxic conditions (21% O_2, 5% CO_2, 12 hours, and 37°C). (**B**) Hypoxic conditions (5% O_2, 5% CO_2, 12 hours, and 37°C). Lens epithelial cells were cultured and immunolabeled. (**C**) The number of junctional Cx43 plaques per cell in normoxic (CNT, control) and hypoxic (HPX) conditions. Data are plotted as the mean ± SD ($n = 3$). No significant difference between HPX and control was found.

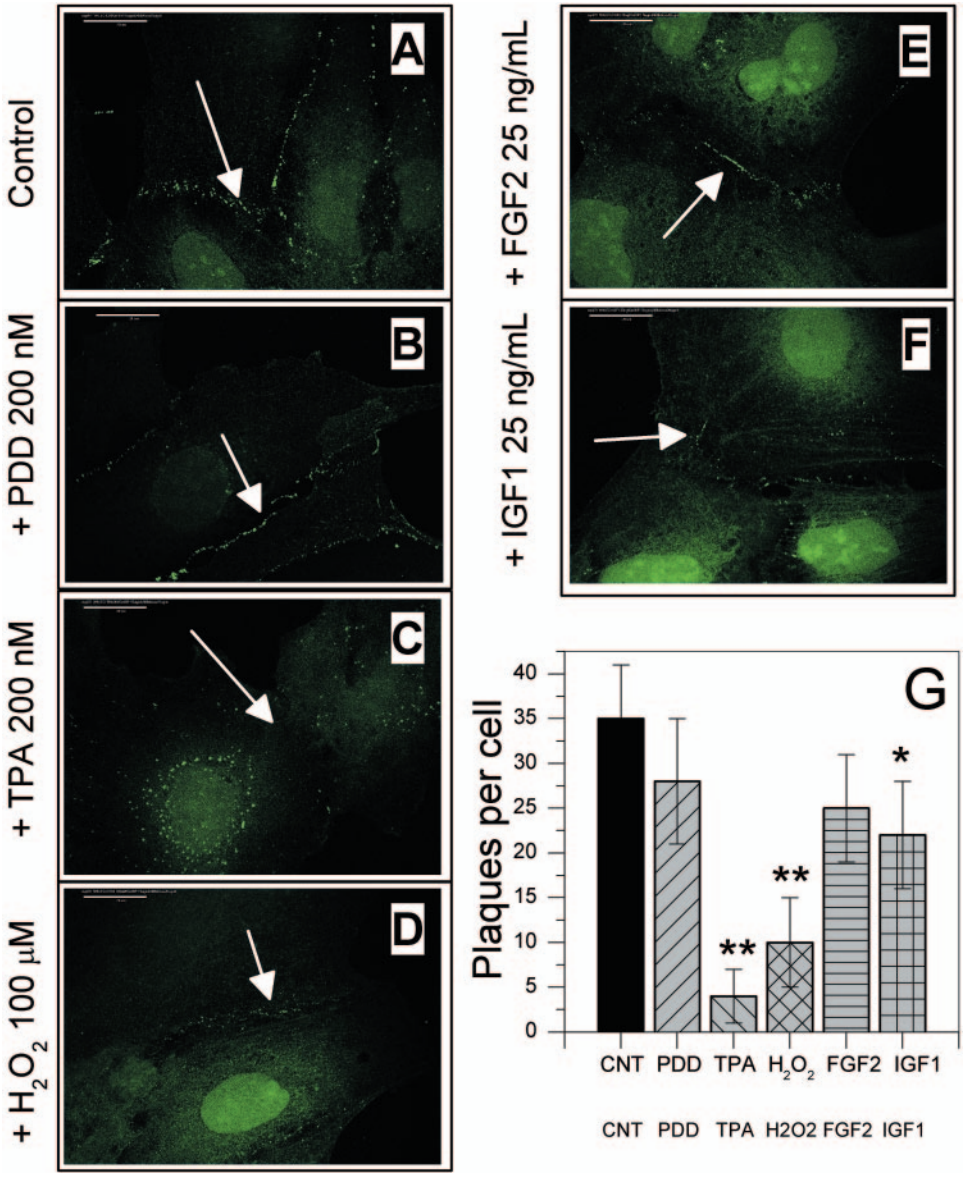

FIGURE 5. (**A–F**) Confocal images of immunolabeled Cx43 (*green*). Lens epithelial cells were starved for 4 hours without serum then treated with TPA (200 nM, 30 minutes, and 37°C), H_2O_2 (100 μM, 30 minutes, and 37°C), FGF-2 or IGF-1 (25 ng/mL, 30 minutes, and 37°C) in normoxic conditions and immunolabeled. PDD (200 nM, 30 minutes, and 37°C) was used as a negative control for TPA treatment. *White arrows*: the junctional interface between two cells. Scale bar, 20 μm. (**G**) Quantitative analyses of Cx43 plaques per cell. Data are plotted as the mean ± SD ($n = 4$). Significant differences: $^{*}P < 0.05$; $^{**}P < 0.001$ between the indicated data and the control.

epithelial cells,[57–59] we performed confocal microscopy studies to investigate whether hypoxia affects Cx43 junctional plaques.

Effects of Hypoxia and PKCγ on Junctional Cx43

In normoxic conditions Cx43 is found at the junctional interface between lens epithelial cells (Fig. 4A). Treatment of cells with hypoxia (1% up to 24 hours) did not affect junctional Cx43 plaques (Fig. 4B). Statistical analyses of the number of junctional Cx43 plaques demonstrated that hypoxia did not affect the number of junctional Cx43 plaques (Fig. 4C). These results demonstrate that lens junctional Cx43 is not regulated by hypoxia; the absence of changes in the number of Cx43 junctional plaques directly support data that hypoxia does not affect dye transfer in the lens epithelial cells. Hypoxia-induced activation of the PKCε may not be related to the regulation of the junctional Cx43, in contrast to the heart. Previously, we demonstrated that among different PKCs, PKCγ, activated by different stress factors such as oxidative stress, phorbol ester, or growth factors (FGF2, IGF1), is the main regulator of junctional Cx43.[44,54,57,60,61] We compared the effect of hypoxia with the effects of these stress and growth factors on junctional Cx43 by using confocal microscopy. Figure 5 shows that very well known activators of PKCγ such as TPA, H_2O_2 and IGF-1 induce the disappearance of junctional Cx43 (Figs. 5C, 5D, 5F, 5G). TPA, IGF1, and H_2O_2 use the same mechanism of PKCγ activation through the C1B domain of PKCγ followed by interaction of activated PKCγ with Cx43.[44,54,57] Treatment of cells with FGF-2 in normoxic conditions did not affect junctional Cx43 (Fig. 5E). We have previously demonstrated that FGF2 is not an activator of PKCγ or PKCε in the lens epithelial cells[62] and therefore serves as a negative control as well as PDD. To prove that hypoxia activates only PKCε and that TPA, H_2O_2, and IGF1 activate only PKCγ in the lens epithelial cells, we performed enzyme assays.

Effect of Hypoxia on PKCε and PKCγ

Treatment of cells with hypoxia (1%–5% O_2, 5% CO_2, and 37°C for 12 hours) resulted in significant activation of PKCε and had no statistically significant effect on PKCγ activity (Fig. 6A). Considering that hypoxia is the natural state of the lens[1–3] and our previous data that PKCε is activated in the fresh lens,[50] we confirmed the activation of PKCε by detecting phosphorylated PKCε on Ser-729 in the whole lens lysates (Figs. 6B, 6C). Thus, we conclude that normoxic conditions inhibit the activity of PKCε and therefore, PKCε would be fully active in the lens

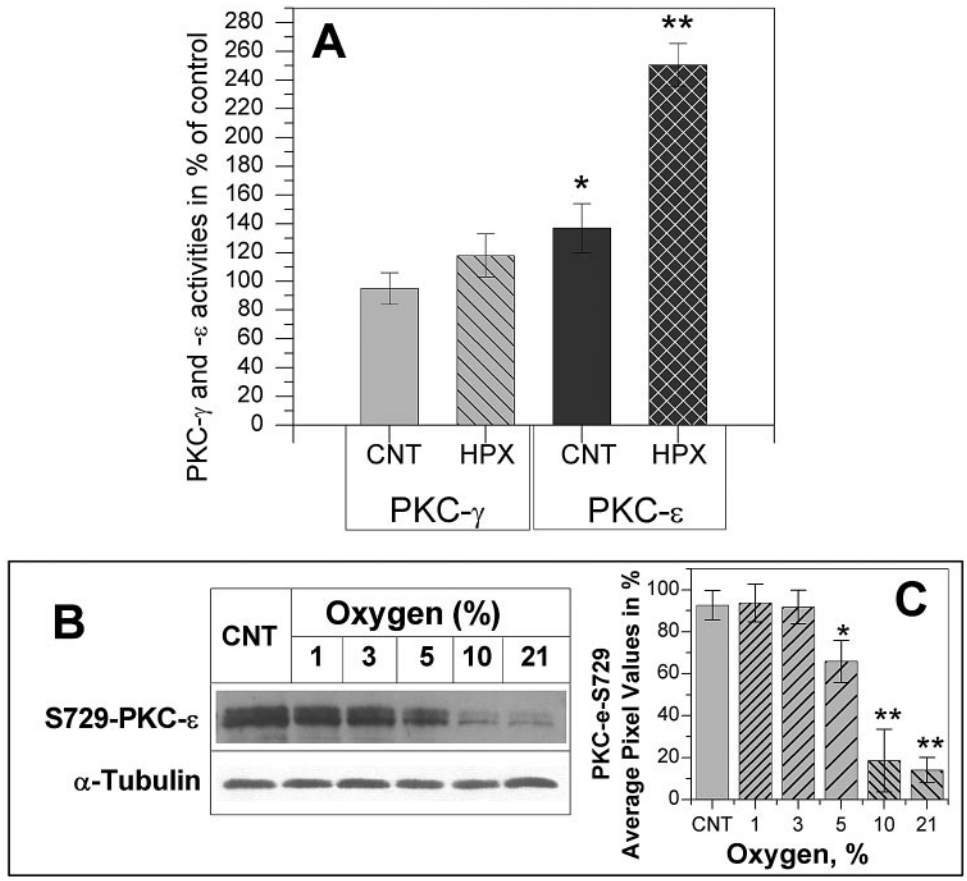

FIGURE 6. (**A**) PKC-γ and -ε enzyme activities in the cell lysates in normoxic (CNT, 20% O_2, 5% CO_2, and 37°C) and hypoxic (HPX) conditions (5% O_2, 5% CO_2, 37°C, and 12 hours). Each PKC was immunoprecipitated from cell lysates, and enzyme activity was assayed. (**B**) Western blot analyses of Ser729-PKCε in lens homogenates of freshly isolated wild-type lenses (CNT) and lenses after hypoxia treatment. Hypoxia (1%–3% of oxygen) does induce the phosphorylation of PKCε on Ser729, an indication of PKCε activation, to the level close to that in the control fresh lenses. α-Tubulin was used as the loading control. (**C**) The average pixel values for every Ser729-PKCε band were calculated and then normalized and plotted in percentage of control (CNT) value obtained for freshly isolated lenses (mean ± SD, $n = 3$). Significant differences: $^{*}P < 0.05$; $^{**}P < 0.001$ between the indicated data and the control.

unless exposed to increased oxygen. Such a condition could occur during surgery or in postvitrectomy surgery,[6] and that type of hypoxia-induced activation of PKCε does not have an effect on junctional Cx43 (Fig. 4).

Effects of TPA, IGF-1, and H_2O_2 on PKCγ and -ε

To investigate which PKC is responsible for the disassembly of junctional Cx43 after treatments with TPA, H_2O_2, IGF-1, and FGF-2, individual PKC enzyme activities were measured. Figure 7A demonstrates that whereas PKCγ was activated by TPA, IGF1, and H_2O_2, the activity of the PKCε was decreased by the same treatments (Fig. 7B) in vitro. Treatment with FGF2 did not change activities of either PKCε or PKCγ. We have demonstrated that FGF2 is not an activator of PKCγ or PKCε in the lens epithelial cells[59] and therefore serves as a negative control. The greatest difference was observed with H_2O_2 treatment, an oxidative stress signal that has been reported to activate cardiac PKCε but not PKCγ.[30] Although PKCγ was activated by H_2O_2 to 180% of control (100 μM, 30 minutes), the activity of the PKCε was decreased, using the same treatments, to only 20% of control. This result demonstrates opposite control mechanism for these two PKC isoforms in lens epithelial cells. Furthermore, it demonstrates that when both isoforms are present in the same cell, the control of these two PKCs differs. This finding further suggests a mechanism for H_2O_2-induced death via PKCε inhibition by H_2O_2, resulting in decreased mitochondria protection.

Removal of PKCε by TPA-Enhanced Interaction of PKCγ with Cx43

To investigate whether there is an interaction between PKCε and Cx43 and whether the inhibition of PKCε activity by normoxia and TPA affected the interaction of PKCε with Cx43, we tested the ability of Cx43 to coimmunoprecipitate with each PKC. TPA, IGF1, and H_2O_2 use the same mechanism of PKCγ activation through the C1B domain of PKCγ followed by interaction of activated PKCγ with Cx43.[44,54,57] We used TPA as a classic example of a PKCγ activator to test how the activation of PKCγ and inhibition of PKCε (as shown in Fig. 7A, 7B) affect their interactions with Cx43. As it is shown in Figure 8, in normoxic conditions, without TPA stimulation, PKCε is associated with Cx43, but not with PKCγ (Fig. 8A). Moreover, PKCε does not coimmunoprecipitate with PKCγ in normoxic conditions (Figs. 8B, 8C) either with or without TPA. TPA treatment induced the dissociation of the PKCε-Cx43 complex and enhanced the interaction of Cx43 with PKCγ (Fig. 8A). These results demonstrate the opposite interactions of each PKC isoform with Cx43 and that further inhibition of the PKCε leads to dissociation of the PKCε-Cx43 complex. Considering that PKCε may exist in two pools: one is Cx43-associated, and another is CytCOxIV-associated[50] The dissociation of the PKCε–Cx43 complex and the inhibition of the PKCε in the PKCε–CytCOxIV complex may contribute to H_2O_2-induced cell death.

Effect of TPA, IGF-1, and H_2O_2, Activators of PKCγ, on Phosphorylation of S368 on Cx43

To demonstrate that activation of PKCγ by TPA, H_2O_2, and IGF1 results in phosphorylation of Cx43, generally considered a main regulatory mechanism for Cx43 (for review, see Ref. 47), we studied phosphorylation of Cx43. Figure 9A demonstrates that patterns of Cx43 phosphorylation, including NP-P1-P2 phosphoisoforms of Cx43, are increased after PKCγ activation by TPA and IGF1 but not after treatment by FGF2. Treatment with H_2O_2 increased the P2 isoform of Cx43. Figure 9B demonstrates Western blot analyses of Cx43, phosphory-

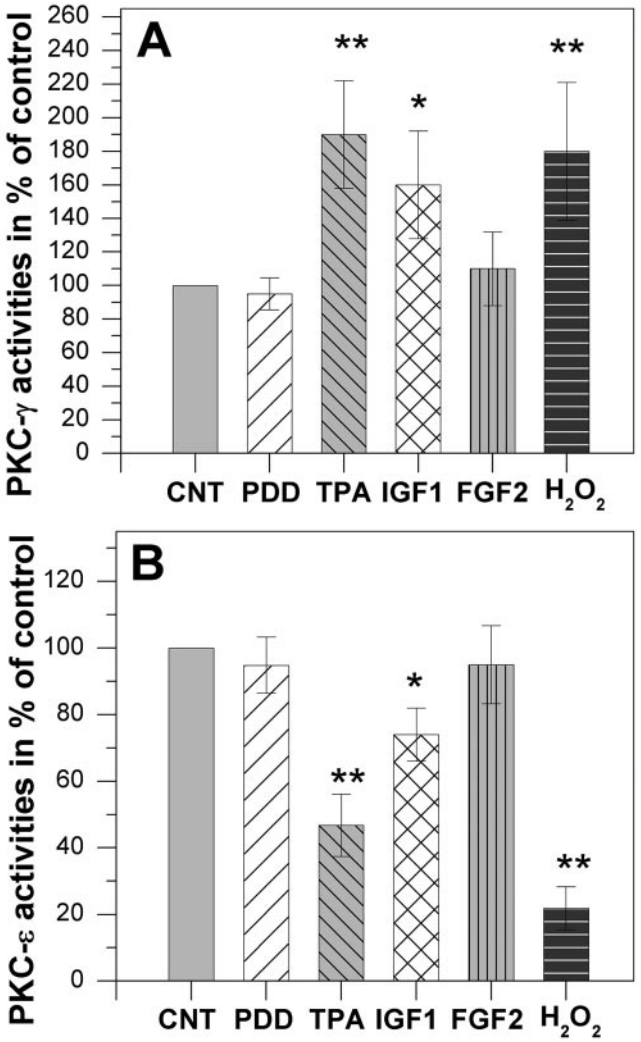

FIGURE 7. (**A**) PKCγ and (**B**) PKCε enzyme activities in the cell lysates in normoxic conditions (21% O_2, 5% CO_2, and 37°C). Control (CNT) lens epithelial cells. Cells were starved for 4 hours without serum and then treated with PDD (200 nM), TPA (200 nM), FGF-2 (25 ng/mL), IGF-1 (25 ng/mL), or H_2O_2 (100 μM) for 30 minutes at 37°C in normoxic conditions. Each PKC was immunoprecipitated from cell lysates, and enzyme activity was assayed. PDD was used as a negative control for TPA treatment. Data are plotted as the percentage of control for each enzyme (mean ± SD, $n = 3$). Significant differences: $^*P < 0.01$; $^{**}P < 0.001$ between indicated data and the control.

lated on Ser-368, detected by anti-Ser-368-Cx43-specific antibodies. Short-term activation of PKCγ by TPA (200 nM, 30 minutes, 37°C) produced a very strong signal from Cx43 due to phosphorylation on Ser-368. Other PKCγ activators such as IGF1 or H_2O_2 also induced phosphorylation on Ser-368 Cx43 but to a lesser extent; FGF-2 had no effect (Fig. 9B). These results demonstrate that agents that activate PKCγ, but inhibit PKCε, have distinct effects on the phosphorylation of Cx43 and distribution of the NP, P1, and P2 isoforms of Cx43 that explain their effect on junctional Cx43 (Fig. 5).

Hypoxia-Induced Degradation or Phosphorylation of Cx43 on Ser368

To study the possible effects of hypoxia on Cx43 levels on phosphorylation, we determined the level of phosphorylation of Ser-368, a well-established phosphorylation site for PKCγ. TPA, used as a positive control, showed a strong stimulation of Cx43 phosphorylation on Ser-368 (Figs. 9B, 10A). Figure 10A shows that hypoxia had no effect on Ser-368 phosphorylation of Cx43 (up to 12 hours). The absence of Ser-368 phosphorylation was not a result of the downregulation of Cx43 or PKCγ. As shown in Figure 10, hypoxia had no effect on the level of total Cx43, PKCε, or PKCγ (Figs. 10B–E). Hypoxic conditions did not decrease the total amount of Cx43 protein, as determined by reacting with anti-Cx43-C-terminal antisera (Fig. 10B) or anti-N-terminal (Fig. 10C) Cx43 antibodies. Western blot analysis with anti-C-terminal Cx43 antibodies also demonstrated that there was no clipping of the C terminus of Cx43 (Fig. 10B). Finally, Figure 11 demonstrates that the appearance of phosphorylation due to TPA activation of PKCγ was not altered by hypoxia. In fact, activation of PKCγ and interaction with and phosphorylation on Cx43 occur regardless of oxygen concentration. These results demonstrate the absolute requirement of PKCγ activation, not PKCε, to convey regulatory control on Cx43 in lens epithelial cells in response to these signals.

DISCUSSION

Our present study demonstrates that hypoxia has a profound effect on the transparency of the lens. One mechanism that underlies this phenomenon is hypoxia-induced activation of PKCε. Previously, we demonstrated that hypoxia activates lens's CytCOxIV and this activation depends on PKCε activation during hypoxia.[50] Our data demonstrated that the absence of PKCε in the KO lens results in fast opacification even in relatively minor oxygen exposure. Our general conclusion is that PKCε is necessary for the protection of lenses from opacity induced by elevated levels of oxygen in the lens. This necessity is further demonstrated by the activation of PKCε in response to lowered oxygen, as observed in whole lens (Figs. 6B, 6C). Our hypothesis is that the high level of opacification in the PKCε-KO lens resulted: first, from the loss of PKCε-dependent activation of the CytCOxIV[50] and, second, from loss of Cx43-PKCε interactions in the absence of PKCε in the PKCε-KO mice. Further work is needed to establish how PKCε acts on Cx43. There could be two pools of PKCε, one that remains to help regulate Cx43 and one that is able to translocate to mitochondria. A similar situation has been found in the heart. It has been shown that PKCε knockout mice do not develop tolerance to ischemia, and mice that express constitutively active PKCε demonstrate increased adenosine nucleotide translocase activity, decreased cytochrome *c* release, and stabilization of the inner mitochondrial membrane potential.[34,37,63] It is important to note that the opacification detected in our experiments originated from the equatorial region and was always cortical. Taking into account that PKCε was found in the lens epithelium and cortex but not in the nucleus of the mouse lens,[50] that the same regions contain almost all lens mitochondria and CytCOxIV and are responsible for almost 90% of oxygen consumption in the lens,[2] that normoxic conditions inhibit the activity of PKCε and therefore PKCε would be fully active in the lens unless exposed to increased oxygen. We believe that our hypothesis about the protective role of PKCε against opacification is logical. This correlation is worth further investigation in the future, considering that elevated oxygen conditions could occur during surgery or in postvitrectomy surgery in the lens.[6] Together with other previously published data,[1–7] our data support the hypothesis that hypoxia is a physiologically normal state for the lens, and any conditions close to normoxia would promote opacification. Thus, the first question is why the oxygen-rich environment of the heart exploits only PKCε, whereas the naturally hypoxic lens utilizes both stress-sensing kinases: PKCγ and PKCε. The most likely answer is that both kinases in the lens serve as protecting mechanisms through different pathways, ensuring double protection against hypoxic and

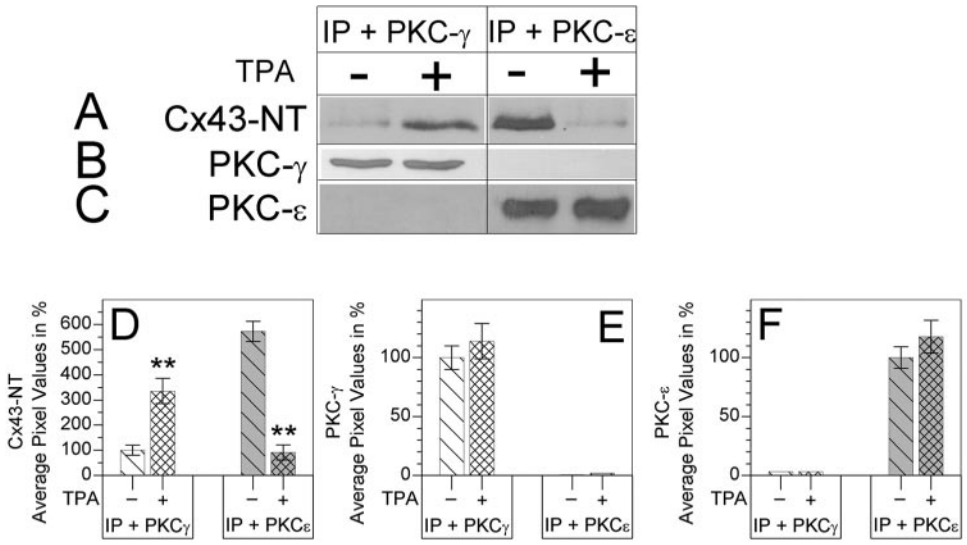

FIGURE 8. Western blot analyses of Cx43 (**A**, **D**), PKCγ (**B**, **E**), and PKCε (**C**, **F**) in immunoprecipitates (IP) with anti-PKCγ or anti-PKCε- antibodies in normoxic (21% O_2, 5% CO_2, and 37°C) conditions. Control (CNT); TPA treatment (+TPA; 200 nM, 30 minutes, and 37°C). Data are plotted as a percentage of the control (mean ± SD, $n = 4$). $^{**}P < 0.001$; significant difference between the indicated data and the control.

oxidative damages in the lens.[10] PKCγ would be activated by H_2O_2 oxidative stress, resulting in inhibition of gap junctions and would remain responsive regardless of oxygen level. PKCε on the other hand may always be active in the hypoxic lens and may usually be active in its mitochondria pool. However, our new data indicating inhibition of PKCε by H_2O_2 suggests a role for PKCε inhibition in lens apoptosis as well.

Does PKCε participate in the regulation of Cx43 gap junctions in the lens epithelial cells as it does in the heart? In the heart, Cx43 complexes with PKCε, but not with PKCγ, and plays an important role in the cardiac ischemic and pharmacologic preconditioning phenomena.[12] Connexin 43 is very important for normal electrophysiological properties of the heart[64,65] which allows PKCε to phosphorylate Cx43 and thus regulate the intercellular communications between cardiac myocytes. It has been found that hypoxia induces dephosphorylation of Cx43 at heart gap junctions; Cx43 has also been found to be downregulated and displaced from intercalated discs.[14,16,21,66,67] These changes were directly associated with uncoupling of gap junctions and decreased electrophysiological properties of cardiomyocytes.[67] Detailed studies of phosphorylation of Cx43 during hypoxia have shown that Ser-297, -306, -330, and -368 at Cx43 are dephosphorylated.[16] Other studies demonstrated that, during hypoxia and preconditioning, PKCε controls the phosphorylation of multiple serines in the C terminus of Cx43 (Ser-365, -368, -369, -372, and -373).[68] In contrast to the cardiomyocytes, our experiments demonstrated a lack of some effects of PKCε on Cx43. Hypoxia did not affect intercellular communication as measured by dye transfer. This opposite regulation has several implications. PKCγ would only regulate gap junctions in response to growth signals and oxidative stress. In normoxic conditions, when the activity of the PKCε is decreased, PKCε is still bound to Cx43, and PKCγ requires either an IGF-1 or oxidative signal to become activated and to interact with and phosphorylate Cx43. In hypoxic conditions, whereas PKCε is activated, only PKCγ-activating signals can induce phosphorylation of Cx43. This activation of PKCγ then displaces PKCε from Cx43 and the activated PKCγ phosphorylates Cx43, especially on Ser-368, regardless of oxygen concentration, causing plaque disassembly and inhibition of the dye transfer. The absence of changes in dye transfer, total amount of Cx43, absence of phosphorylation on Ser-368, the absence of P1 or P2 phosphoisoforms of Cx43 explain why hypoxia itself does not inhibit the intercel-

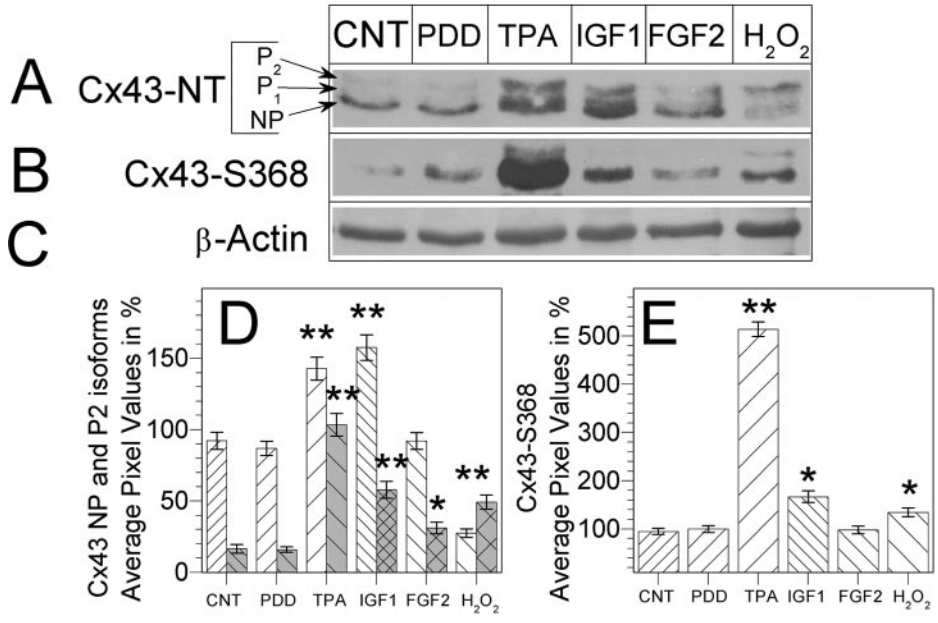

FIGURE 9. Western blot analyses of cell lysates in normoxic conditions. (**A**, **D**) Cx43, nonphosphorylated (NP) Cx43 isoform. P1 and P2, phosphoisoforms of Cx43. (**D**; *open patterned bars*) NP phosphoisoform; (*gray bars*) P2 phosphoisoform of Cx43. (**B**, **E**) Ser-368-phosphoisoform of Cx43. There was no shift in the relative molecular weight of the S368-Cx43. When compared with positions of the NP, P1, and P2 bands in (**A**), S368-Cx43 migrated at the position of the NP. Control (CNT). Cells were treated with PDD (200 nM), TPA (200 nM), FGF-2 (25 ng/mL), IGF-1 (25 ng/mL), or H_2O_2 (100 μM) for 30 minutes at 37°C in normoxic conditions. (**C**) β-Actin was used as the loading control. Data are plotted as percentage of control (mean ± SD, $n = 4$). Significant difference: $^{*}P < 0.01$, $^{**}P < 0.001$, between indicated data and control; only statistically relevant data were marked.

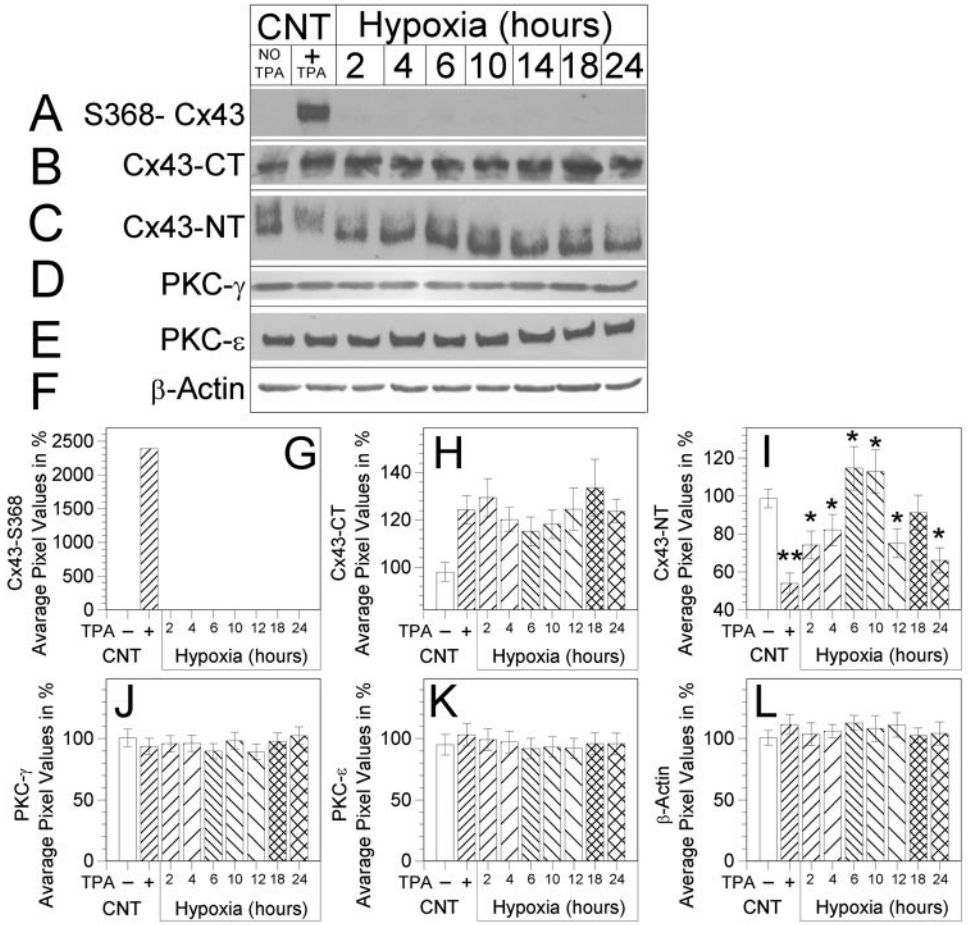

FIGURE 10. Western blot analyses of cell lysates in normoxic conditions (CNT, No TPA, + TPA) conditions and in hypoxia (5% O_2, 5% CO_2, and 37°C). (**A**, **G**) Ser-368-phosphoisoform of Cx43, (**B**, **H**) Cx43 probed by anti-C-terminal-Cx43 antiserum and (**C**, **I**) Cx43 probed by anti-N-terminal-Cx43 antiserum. Western blot analyses of PKCγ (**D**, **J**) and PKCε (**E**, **K**). TPA treatment (200 nM, 30 minutes, and 37°C) was used as the positive control for phosphorylation of Cx43 on Ser-368 (**A**). (**F**, **L**) β-Actin was used as the loading control. Data are plotted as a percentage of control (mean ± SD, $n = 4$). Significant difference: $^{*}P < 0.01$; $^{**}P < 0.001$ between indicated data and control; only statistically relevant data are marked.

lular communication and does not affect gap junctional plaques. Our data led us to the conclusion that, in the case of lens epithelial cells, PKCε does not participate in the regulation of disassembling and degradation of Cx43 gap junction plaques. That role is a specific one for PKCγ. In contrast, degradation is accomplished in the heart by PKCε.[35]

But the question remains: What is the purpose of PKCε if it does not participate in the regulation of gap junctions? In conditions of hypoxia which activates PKCε in heart and in the lens, the PKCε, in the heart, is translocated to plasma membranes[27,69,70] and phosphorylates and inhibits Cx43 gap junctions,[35,71] to prevent the propagation of apoptotic signal.[34] In

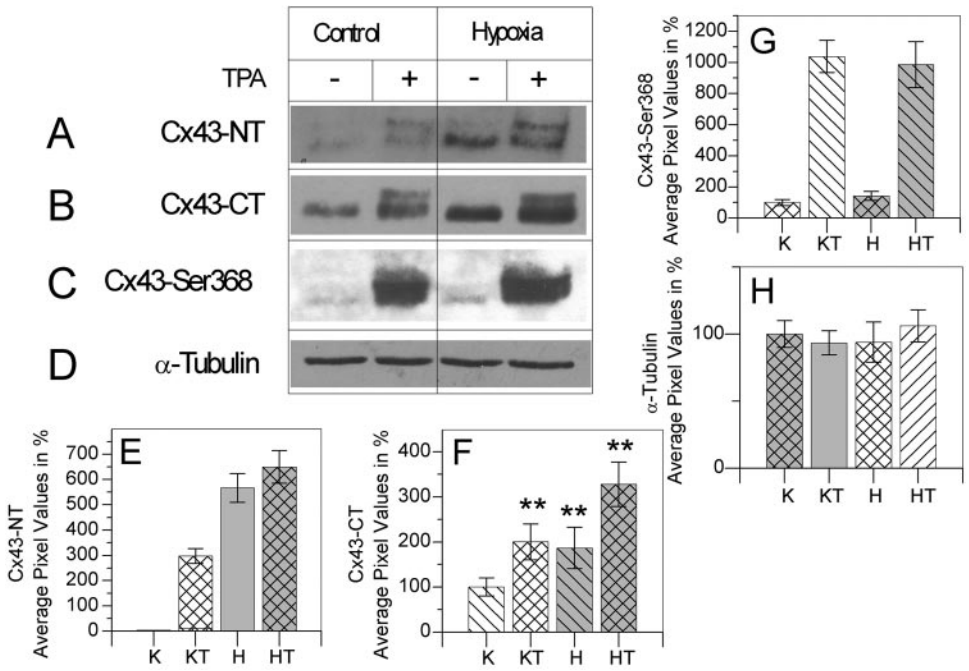

FIGURE 11. Western blot analyses of Cx43 probed by (**A**, **E**) anti-N-terminal-Cx43 antibodies, (**B**, **F**) anti-C-terminal-Cx43, (**C**, **G**) anti-Ser-368-Cx43 antibodies in cell lysates in normoxic (CNT, 21% O_2, 5% CO_2, and 37°C) conditions and in 12 hours of hypoxia (5% O_2, 5% CO_2, and 37°C). TPA treatment (200 nM, 30 minutes, and 37°C) was performed. In the case of hypoxia+TPA, 200 nM was added directly to the media after 12 hours of hypoxia and incubated for 30 minutes at 37°C in the same hypoxic conditions. (**D**, **H**) α-Tubulin was used as the loading control. Data are plotted as a percentage of the control (mean ± SD, $n = 4$). $^{**}P < 0.001$, difference between the indicated data and the control.

lens, PKCε, activated by hypoxia, translocates to the mitochondria, protects CytCOxIV and blocks apoptosis, by a mechanism which is likely similar to that in the heart.[72] Both pathways, PKCε-dependent and PKCγ-dependent, work in conjunction, preventing mitochondrial CytCOxIV from damage, and, keeping communication between adjacent epithelial cells open through junctional Cx43 (the bystander effect). This hypothesis is also supported by our recent data demonstrating that mutations in the Zn-finger of the C1B stress switch domain of PKCγ removes PKCγ from the regulation of Cx43 gap junctions, induces an increased amount of unregulated Cx43 plaques and promotes caspase-3-based apoptosis in the lens epithelial cells through open Cx43 channels.[49] In lens that expresses both isoforms, PKCγ appears to be the primary regulator of gap junctions in response to oxidative stress. PKCγ displaces PKCε from gap junctions as a means of protection that is not required in the more resilient tissues such as heart. In the hypoxic lens, PKCε would be primarily found in the mitochondria, to be used as an adaptive/protective response to natural hypoxia. Although knockout mouse models exist for both PKCγ and PKCε, a double-knockout does not exist, and this would be an ideal model to determine the requirements for these two stress-sensing kinases.

References

1. Beebe DC. Maintaining transparency: a review of the developmental physiology and pathophysiology of two avascular tissues. *Semin Cell Dev Biol.* 2008;19:125–133.
2. McNulty R, Wang H, Mathias RT, Ortwerth BJ, Truscott RJ, Bassnett S. Regulation of tissue oxygen levels in the mammalian lens. *J Physiol.* 2004;559:883–898.
3. Shui YB, Fu JJ, Garcia C, et al. Oxygen distribution in the rabbit eye and oxygen consumption by the lens. *Invest Ophthalmol Vis Sci.* 2006;47:1571–1580.
4. Shui YB, Beebe DC. Age-dependent control of lens growth by hypoxia. *Invest Ophthalmol Vis Sci.* 2008;49:1023–1029.
5. Holekamp NM, Shui YB, Beebe D. Lower intraocular oxygen tension in diabetic patients: possible contribution to decreased incidence of nuclear sclerotic cataract. *Am J Ophthalmol.* 2006;141:1027–1032.
6. Holekamp NM, Shui YB, Beebe DC. Vitrectomy surgery increases oxygen exposure to the lens: a possible mechanism for nuclear cataract formation. *Am J Ophthalmol.* 2005;139:302–310.
7. Helbig H, Hinz JP, Kellner U, Foerster MH. Oxygen in the anterior chamber of the human eye. *Ger J Ophthalmol.* 1993;2:161–164.
8. Whikehart DR. *Biochemistry of the Eye.* 2d ed. Boston: Butterworth-Heinemann; 2003.
9. Winkler BS, Riley MV. Relative contributions of epithelial cells and fibers to rabbit lens ATP content and glycolysis. *Invest Ophthalmol Vis Sci.* 1991;32:2593–2598.
10. Barnett ME, Madgwick DK, Takemoto DJ. Protein kinase C as a stress sensor. *Cell Signal.* 2007;19:1820–1829.
11. Boengler K, Konietzka I, Buechert A, et al. Loss of ischemic preconditioning's cardioprotection in aged mouse hearts is associated with reduced gap junctional and mitochondrial levels of connexin 43. *Am J Physiol Heart Circ Physiol.* 2007;292:H1764–H1769.
12. Inagaki K, Churchill E, Mochly-Rosen D. Epsilon protein kinase C as a potential therapeutic target for the ischemic heart. *Cardiovasc Res.* 2006;70:222–230.
13. Solan JL, Marquez-Rosado L, Sorgen PL, Thornton PJ, Gafken PR, Lampe PD. Phosphorylation at S365 is a gatekeeper event that changes the structure of Cx43 and prevents down-regulation by PKC. *J Cell Biol.* 2007;179:1301–1309.
14. Lampe PD, Cooper CD, King TJ, Burt JM. Analysis of Connexin43 phosphorylated at S325, S328 and S330 in normoxic and ischemic heart. *J Cell Sci.* 2006;119:3435–3442.
15. Dhein S. New, emerging roles for cardiac connexins: mitochondrial Cx43 raises new questions. *Cardiovasc Res.* 2005;67:179–181.
16. Axelsen LN, Stahlhut M, Mohammed S, et al. Identification of ischemia-regulated phosphorylation sites in connexin43: a possible target for the antiarrhythmic peptide analogue rotigaptide (ZP123). *J Mol Cell Cardiol.* 2006;40:790–798.
17. Zhang SW, Liu SX, Deng LB. Immunohistochemical study of Cx43 dephosphorylation in human left ventricular myocardium suffered by acute ischemia (in Chinese). *Fa Yi Xue Za Zhi.* 2004;20:136–139,142.
18. Daleau P, Boudriau S, Michaud M, Jolicoeur C, Kingma JG Jr. Preconditioning in the absence or presence of sustained ischemia modulates myocardial Cx43 protein levels and gap junction distribution. *Can J Physiol Pharmacol.* 2001;79:371–378.
19. Lerner DL, Yamada KA, Schuessler RB, Saffitz JE. Accelerated onset and increased incidence of ventricular arrhythmias induced by ischemia in Cx43-deficient mice. *Circulation.* 2000;101:547–552.
20. Hatanaka K, Kawata H, Toyofuku T, Yoshida K. Down-regulation of connexin43 in early myocardial ischemia and protective effect by ischemic preconditioning in rat hearts in vivo. *Jpn Heart J.* 2004;45:1007–1019.
21. Schulz R, Gres P, Skyschally A, et al. Ischemic preconditioning preserves connexin 43 phosphorylation during sustained ischemia in pig hearts in vivo. *FASEB J.* 2003;17:1355–1357.
22. Rodriguez-Sinovas A, Cabestrero A, Lopez D, et al. The modulatory effects of connexin 43 on cell death/survival beyond cell coupling. *Prog Biophys Mol Biol.* 2007;94:219–232.
23. Shintani-Ishida K, Uemura K, Yoshida K. Hemichannels in cardiomyocytes open transiently during ischemia and contribute to reperfusion injury following brief ischemia. *Am J Physiol Heart Circ Physiol.* 2007;293:H1714–H1720.
24. Htun P, Ito WD, Hoefer IE, Schaper J, Schaper W. Intramyocardial infusion of FGF-1 mimics ischemic preconditioning in pig myocardium. *J Mol Cell Cardiol.* 1998;30:867–877.
25. Doble BW, Ping P, Kardami E. The epsilon subtype of protein kinase C is required for cardiomyocyte connexin-43 phosphorylation. *Circ Res.* 2000;86:293–301.
26. Srisakuldee W, Nickel BE, Fandrich RR, Jiang ZS, Kardami E. Administration of FGF-2 to the heart stimulates connexin-43 phosphorylation at protein kinase C target sites. *Cell Commun Adhes.* 2006;13:13–19.
27. Ogbi M, Johnson JA. Protein kinase Cepsilon interacts with cytochrome c oxidase subunit IV and enhances cytochrome c oxidase activity in neonatal cardiac myocyte preconditioning. *Biochem J.* 2006;393:191–199.
28. Ogbi M, Wingard CJ, Ogbi S, Johnson JA. Epsilon protein kinase C lengthens the quiescent period between spontaneous contractions in rat ventricular cardiac myocytes and trabecula. *Naunyn Schmiedebergs Arch Pharmacol.* 2004;370:251–261.
29. Ytrehus K, Liu Y, Downey JM. Preconditioning protects ischemic rabbit heart by protein kinase C activation. *Am J Physiol Heart Circ Physiol.* 1994;266:H1145–H1152.
30. Zhang HY, McPherson BC, Liu H, Baman TS, Rock P, Yao Z. H(2)O(2) opens mitochondrial K(ATP) channels and inhibits GABA receptors via protein kinase C-epsilon in cardiomyocytes. *Am J Physiol Heart Circ Physiol.* 2002;282:H1395–H1403.
31. Zhang WH, Lu FH, Zhao YJ, et al. Post-conditioning protects rat cardiomyocytes via PKCepsilon-mediated calcium-sensing receptors. *Biochem Biophys Res Commun.* 2007;361:659–664.
32. Guo D, Nguyen T, Ogbi M, et al. Protein kinase C-epsilon coimmunoprecipitates with cytochrome oxidase subunit IV and is associated with improved cytochrome-c oxidase activity and cardioprotection. *Am J Physiol Heart Circ Physiol.* 2007;293:H2219–H2230.
33. Korzick DH, Kostyak JC, Hunter JC, Saupe KW. Local delivery of PKCepsilon-activating peptide mimics ischemic preconditioning in aged hearts through GSK-3beta but not F1-ATPase inactivation. *Am J Physiol Heart Circ Physiol.* 2007;293:H2056–H2063.
34. Budas GR, Mochly-Rosen D. Mitochondrial protein kinase Cepsilon (PKCepsilon): emerging role in cardiac protection from ischaemic damage. *Biochem Soc Trans.* 2007;35:1052–1054.
35. Hund TJ, Lerner DL, Yamada KA, Schuessler RB, Saffitz JE. Protein kinase Cepsilon mediates salutary effects on electrical coupling induced by ischemic preconditioning. *Heart Rhythm.* 2007;4:1183–1193.

36. Kabir AM, Clark JE, Tanno M, et al. Cardioprotection initiated by reactive oxygen species is dependent on activation of PKCepsilon. *Am J Physiol Heart Circ Physiol.* 2006;291:H1893–H1899.
37. Yu Q, Nguyen T, Ogbi M, Caldwell RW, Johnson JA. Differential loss of cytochrome-c oxidase subunits in ischemia-reperfusion injury: exacerbation of COI subunit loss by PKC-epsilon inhibition. *Am J Physiol Heart Circ Physiol.* 2008;294:H2637–H2645.
38. Ogbi M, Chew CS, Pohl J, Stuchlik O, Ogbi S, Johnson JA. Cytochrome c oxidase subunit IV as a marker of protein kinase Cepsilon function in neonatal cardiac myocytes: implications for cytochrome c oxidase activity. *Biochem J.* 2004;382:923–932.
39. Churchill EN, Mochly-Rosen D. The roles of PKCdelta and epsilon isoenzymes in the regulation of myocardial ischaemia/reperfusion injury. *Biochem Soc Trans.* 2007;35:1040–1042.
40. Vohra HA, Galinanes M. Myocardial preconditioning against ischemia-induced apoptosis and necrosis in man. *J Surg Res.* 2006;134:138–144.
41. Murriel CL, Mochly-Rosen D. Opposing roles of delta and epsilonPKC in cardiac ischemia and reperfusion: targeting the apoptotic machinery. *Arch Biochem Biophys.* 2003;420:246–254.
42. Matsumura K, Komori S, Takusagawa M, et al. Protein kinase C is involved in cardioprotective effects of ischemic preconditioning on infarct size and ventricular arrhythmia in rats in vivo. *Mol Cell Biochem.* 2000;214:39–45.
43. Kuno A, Critz SD, Cui L, et al. Protein kinase C protects preconditioned rabbit hearts by increasing sensitivity of adenosine A2b-dependent signaling during early reperfusion. *J Mol Cell Cardiol.* 2007;43:262–271.
44. Lin D, Takemoto DJ. Oxidative activation of protein kinase Cgamma through the C1 domain; effects on gap junctions. *J Biol Chem.* 2005;280:13682–13693.
45. Lin D, Shanks D, Prakash O, Takemoto DJ. Protein kinase C gamma mutations in the C1B domain cause caspase-3-linked apoptosis in lens epithelial cells through gap junctions. *Exp Eye Res.* 2007;85:113–122.
46. Ek-Vitorin JF, King TJ, Heyman NS, Lampe PD, Burt JM. Selectivity of connexin 43 channels is regulated through protein kinase C-dependent phosphorylation. *Circ Res.* 2006;98:1498–1505.
47. Solan JL, Lampe PD. Connexin phosphorylation as a regulatory event linked to gap junction channel assembly. *Biochim Biophys Acta.* 2005;1711:154–163.
48. Lampe PD, Lau AF. The effects of connexin phosphorylation on gap junctional communication. *Int J Biochem Cell Biol.* 2004;36:1171–1186.
49. Lin D, Takemoto DJ. Protection from ataxia-linked apoptosis by gap junction inhibitors. *Biochem Biophys Res Commun.* 2007;362:982–987.
50. Barnett M, Lin D, Akoyev V, Willard L, Takemoto D. Protein kinase C epsilon activates lens mitochondrial cytochrome c oxidase subunit IV during hypoxia. *Exp Eye Res.* 2008;86:226–234.
51. Behndig A, Karlsson K, Reaume AG, Sentman ML, Marklund SL. In vitro photochemical cataract in mice lacking copper-zinc superoxide dismutase. *Free Radic Biol Med.* 2001;31:738–744.
52. Akoyev V, Takemoto DJ. ZO-1 is required for protein kinase C gamma-driven disassembly of connexin 43. *Cell Signal.* 2007;19:958–967.
53. Nguyen TA, Boyle DL, Wagner LM, Shinohara T, Takemoto DJ. LEDGF activation of PKC gamma and gap junction disassembly in lens epithelial cells. *Exp Eye Res.* 2003;76:565–572.
54. Lin D, Boyle DL, Takemoto DJ. IGF-I-induced phosphorylation of connexin 43 by PKCgamma: regulation of gap junctions in rabbit lens epithelial cells. *Invest Ophthalmol Vis Sci.* 2003;44:1160–1168.
55. Sundset R, Ytrehus K, Zhang Y, Saffitz JE, Yamada KA. Repeated simulated ischemia and protection against gap junctional uncoupling. *Cell Commun Adhes.* 2007;14:239–249.
56. Gothie E, Richard DE, Berra E, Pages G, Pouyssegur J. Identification of alternative spliced variants of human hypoxia-inducible factor-1alpha. *J Biol Chem.* 2000;275:6922–6927.
57. Nguyen TA, Takemoto LJ, Takemoto DJ. Inhibition of gap junction activity through the release of the C1B domain of protein kinase Cgamma (PKCgamma) from 14-3-3: identification of PKCgamma-binding sites. *J Biol Chem.* 2004;279:52714–52725.
58. Lin D, Zhou J, Zelenka PS, Takemoto DJ. Protein kinase Cgamma regulation of gap junction activity through caveolin-1-containing lipid rafts. *Invest Ophthalmol Vis Sci.* 2003;44:5259–5268.
59. Wagner LM, Saleh SM, Boyle DJ, Takemoto DJ. Effect of protein kinase Cgamma on gap junction disassembly in lens epithelial cells and retinal cells in culture. *Mol Vis.* 2002;8:59–66.
60. Zampighi GA, Planells AM, Lin D, Takemoto D. Regulation of lens cell-to-cell communication by activation of PKCgamma and disassembly of Cx50 channels. *Invest Ophthalmol Vis Sci.* 2005;46:3247–3255.
61. Lin D, Lobell S, Jewell A, Takemoto DJ. Differential phosphorylation of connexin46 and connexin50 by H2O2 activation of protein kinase Cgamma. *Mol Vis.* 2004;10:688–695.
62. Wagner LM, Fowler VM, Takemoto DJ. The interaction and phosphorylation of tropomodulin by protein kinase Calpha in N/N 1003A lens epithelial cells. *Mol Vis.* 2002;8:394–406.
63. McCarthy J, McLeod CJ, Minners J, Essop MF, Ping P, Sack MN. PKCepsilon activation augments cardiac mitochondrial respiratory post-anoxic reserve: a putative mechanism in PKCepsilon cardioprotection. *J Mol Cell Cardiol.* 2005;38:697–700.
64. Valiunas V, Beyer EC, Brink PR. Cardiac gap junction channels show quantitative differences in selectivity. *Circ Res.* 2002;91:104–111.
65. Yue Y, Qu Y, Boutjdir M. Protective role of protein kinase C epsilon activation in ischemia-reperfusion arrhythmia. *Biochem Biophys Res Commun.* 2006;349:432–438.
66. Matsushita S, Kurihara H, Watanabe M, Okada T, Sakai T, Amano A. Alterations of phosphorylation state of connexin 43 during hypoxia and reoxygenation are associated with cardiac function. *J Histochem Cytochem.* 2006;54:343–353.
67. Zeevi-Levin N, Barac YD, Reisner Y, et al. Gap junctional remodeling by hypoxia in cultured neonatal rat ventricular myocytes. *Cardiovasc Res.* 2005;66:64–73.
68. Bowling N, Huang X, Sandusky GE, et al. Protein kinase C-alpha and -epsilon modulate connexin-43 phosphorylation in human heart. *J Mol Cell Cardiol.* 2001;33:789–798.
69. Hunter JC, Korzick DH. Protein kinase C distribution and translocation in rat myocardium: methodological considerations. *J Pharmacol Toxicol Methods.* 2005;51:129–138.
70. Wolfrum S, Schneider K, Heidbreder M, Nienstedt J, Dominiak P, Dendorfer A. Remote preconditioning protects the heart by activating myocardial PKCepsilon-isoform. *Cardiovasc Res.* 2002;55:583–589.
71. Dhein S, Polontchouk L, Salameh A, Haefliger JA. Pharmacological modulation and differential regulation of the cardiac gap junction proteins connexin 43 and connexin 40. *Biol Cell.* 2002;94:409–422.
72. Baines CP, Zhang J, Wang GW, et al. Mitochondrial PKCepsilon and MAPK form signaling modules in the murine heart: enhanced mitochondrial PKCepsilon-MAPK interactions and differential MAPK activation in PKCepsilon-induced cardioprotection. *Circ Res.* 2002;90:390–397.